Taylor & Francis
Taylor & Francis Group

ARTICLE

Check for updates

A new rhinocerotid (Mammalia, Rhinocerotidae) from the latest Miocene of Southern Italy

Luca Pandolfi [a], Antonella Cinzia Marra[b], Giuseppe Carone[c], Leonardo Maiorino[d] and Lorenzo Rook [a]

aDipartimento di Scienze della Terra, Università degli Studi di Firenze, Firenze, Italy; bDipartimento di Scienze Matematiche e Informatiche, di Scienze Fisiche e di Scienze della Terra, Università degli Studi di Messina, Messina, Italy; cCivico Museo del Mare di Tropea, Largo Ruffa, Tropea (VV), Italy; dDipartimento di Scienze, Università degli Studi di Roma Tre, Roma, Italy

ABSTRACT

A new species of Rhinocerotidae (Perissodactyla), 'Ceratotherium' advenientis sp. nov., from the late Miocene (8.1–7.2 Ma) locality of Cava Gentile, Calabria (Southern Italy), is described. 'Ceratotherium' advenientis displays morphological characters close to Rhinocerotina, in particular to dicerotines, and can be distinguished from the late Miocene elasmotheres, teleoceratines and aceratheres recorded in Eurasia and Africa. The new taxon clearly differs from the European latest Miocene species Dihoplus schleiermacheri, Dihoplus pikermiensis, 'Dihoplus' megarhinus and Ceratotherium neumayri, and from the African species Ceratotherium douariense, Ceratotherium? primaevum and Paradiceros mukirii. 'Ceratotherium' advenientis also differs from the Chinese dicerotine Diceros gansuensis and from the extant African species. The new taxon is characterized by peculiar features, in particular in the morphology and dimension of the neurocranial portion, and by having a nuchal crest wider than in the extant African rhinoceroses, C. neumayri, C. douariense, and European latest Miocene species. A cladistic analysis places 'Ceratotherium' advenientis in a polytomy with the extant Diceros bicornis, C. neumayri and a small clade composed by C. simum and C. antiquitatis. The African affinities of the new taxon support the Calabrian-Peloritan arc as a northern extension of the African continental shelf during the late Miocene.

Introduction

The late Miocene site of Cava Gentile (Vibo Valentia, Italy) has yielded a fossil mammal assemblage that is extremely informative regarding the complex history of the Tortonian/Messinian land mammals populating the central Mediterranean lands (Marra et al. 2017). Albeit the area was already known for the outstanding record of marine mammals, especially sirenians (Neviani 1886; Del Campana 1924; Moncharmont Zei and Moncharmont 1987; Carone and Domning 2007; Guido et al. 2012; Carone et al. 2013, Marra et al. 2016), the first account of the occurrence of a terrestrial mammal from the area was given by Ferretti et al. (2003), who reported the occurrence of the elephantid Stegotetrabelodon syrticus Petrocchi, 1941. This finding was considered of extreme interest as it was indicative of a land connection between the Cessaniti area (Calabria, southern Italy) and northern Africa. This evidence, in fact, increased our knowledge of the complex late Miocene palaeobiogeography of Italy, where two distinct palaeobioprovinces, the Tusco-Sardinian and the Abruzzi-Apulian, both affected by remarkable insularity, have been well recognised (Rook et al. 2006). The land mammal assemblage from the Cessaniti area actually documents a third bioprovince in the central Mediterranean that differs completely from the previous ones and is characterised by a mixture of North-African/Pikermian affinities. In addition to the elephantid Stegotetrabelodon syrticus (Ferretti et al. 2003), other terrestrial mammals recovered from Cessaniti include two giraffid species, Samotherium cf.

boissieri Forsyth-Major, 1888 and Bohlinia cf. attica Matthew, 1929 (Marra et al. 2011), and a boselaphine bovid, Tragoportax cf. rugosifrons (Schlosser 1904) (Marra 2018). The occurrence of a rhinoceros within the Cessaniti assemblage has been reported in several papers (Marra et al. 2011, 2017; Pandolfi and Rook 2017), but never described in detail. Rook et al. (2006) listed the presence of 'Diceros' primaevus, whilst Marra et al. (2011, 2017) cautiously referred the few rhinoceros remains from Cava Gentile to Diceros (comparable to 'Diceros' primaevus or 'Diceros' neumayri). Recently, Pandolfi and Rook (2017) suggested a provisional attribution as Rhinocerotinae indet. pending a detailed study of the material.

The aim of the present paper is to describe the Rhinocerotidae skull from Cava Gentile, to precise its systematic and phylogenetic affinities, as well as the paleogeographic significance of this new element within the Cessaniti land mammal assemblage.

Stratigraphic and chronologic context

The site of Cessaniti is located within the Capo Vaticano – Monte Poro sedimentary basin in the south-western sector of the Calabria-Peloritani Arc (Figure 1). The basin overlies a crystalline substratum, Paleozoic in age, and is characterized by a stratigraphic succession attributable to late Miocene, which outcrops with different thickness and facies throughout the area (Nicotera 1959; Gramigna et al. 2012).
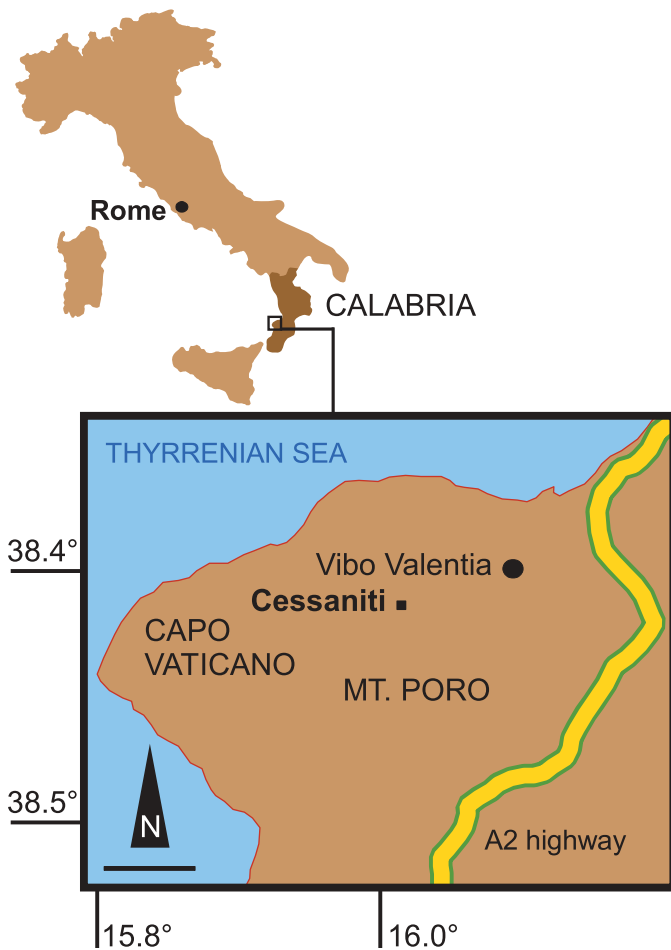

Figure 1. Geographic position of the fossiliferous locality of Cava Gentile, Cessaniti, Italy.

At Cessaniti, quarry works at Cava Gentile have exposed the complete stratigraphic sequence in its maximum thickness (Figure 2) and allowed releasing most of the Cessaniti rich paleontological record. The Cava Gentile succession has been recently described and interpreted as the result of a complex sedimentary evolution of the sedimentary basin (Marra et al. 2017). The stratigraphic and sedimentological study of the section evidenced an overall transgressive trend within the Late Tortonian succession, punctuated by minor episodes of forced regression, as attested by soils and fluvial deposits intercalated within the Cava Gentile succession. As a consequence, the relative sea level rises that characterised this sedimentation patterns allowed accumulation of marine and terrestrial fossils in specific transgressive horizons.

The combination of palaeomagnetic data and biostratigraphic analyses, together with the biochronological constraints offered by the Cessaniti mammal assemblage, allows the chronological framing of the succession. The basal unit of the Cessaniti succession is attributed to the normal Chron C4n (8.1–7.5 Ma), while the calcareous nannofossil assemblages present in the samples from the top of the succession indicate a biozone (CNM17) at the Tortonian/Messinian
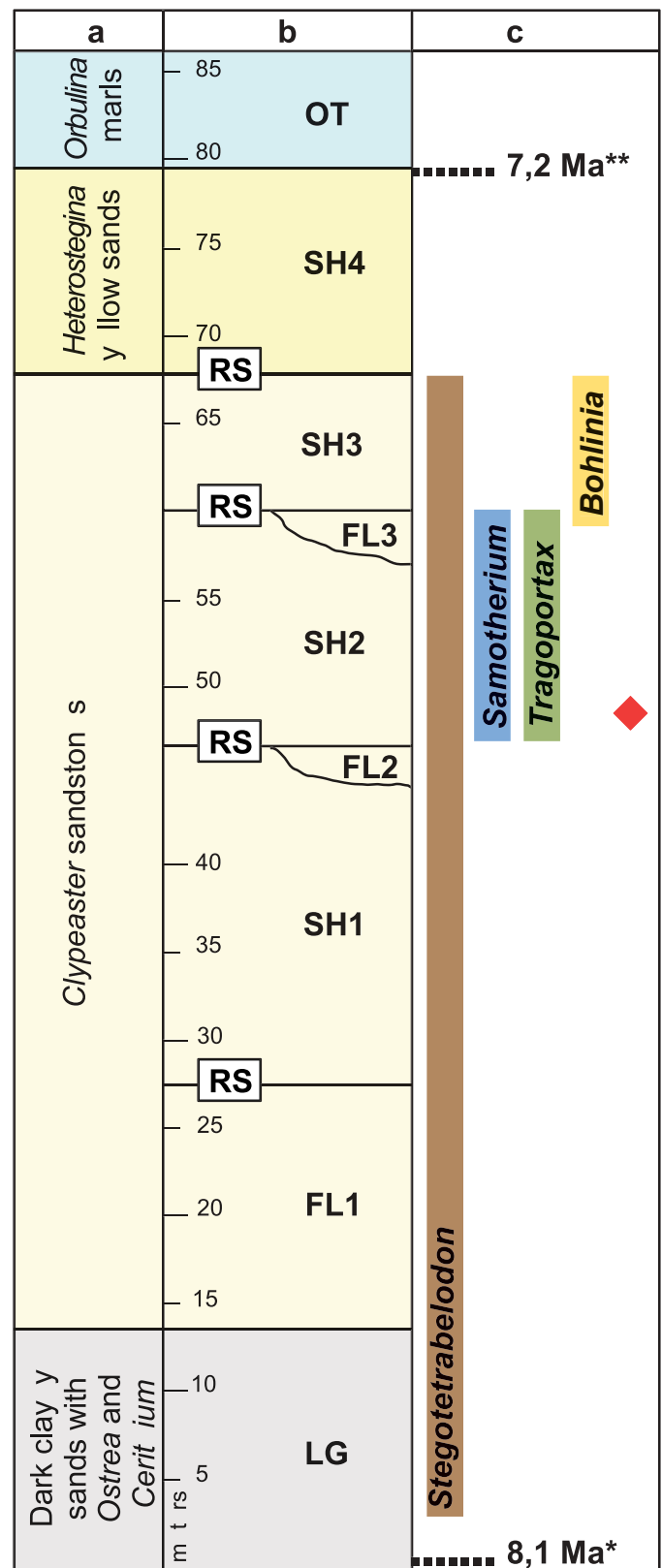

Figure 2. Schematic stratigraphy of Cava Gentile (Cessaniti, southern Italy) with land mammal occurrences: (a) Informal stratigraphy (according to Nicotera 1959; Ogniben 1973; Rao et al. 2007); (b) Stratigraphy according to Marra et al. (2017) (LG: Lagoonal deposits, FL: fluvial deposits, SH: shoreface deposits, OT: offshore transition; RS: ravinement surface); c) Occurrences of mammalian taxa; *) dating by the attribution of LG to Chron C4n (Marra et al. 2017); **) dating by the attribution of OT to nannoplankton zone CNM17 (Marra et al. 2017); red rombus indicates the level where the GPT rhinocerotid has been collected CES.

transition. The maximum range of the Cessaniti land mammal assemblage from Cava Gentile is therefore about 1 Ma, bracketed between 8.1 and 7.2 Ma (Marra et al. 2017).

Late Miocene Rhinocerotina of the Mediterranean Basin: a short overview

Late Miocene Rhinocerotina Gray, 1821 (= Rhinocerotini sensu Heissig 1999) are relatively common and well-known in Europe and Anatolia.

Dihoplus schleiermacheri (Kaup 1832) occurred from MN 9 to MN 12 mammal zones at several central and western European localities and it was the sole Rhinocerotina species in western Europe during the latest Miocene (Kaup 1832; Guérin 1980; Cerdeño 1992; Heissig 1996, 1999; Pandolfi 2018). *Dihoplus pikermiensis* (Toula 1906) occurred in the latest Vallesian and Turolian deposits (MN 10-MN 13) of the Balkan Peninsula and Turkey (Geraads 1988; Heissig 1999; Antoine and Saraç 2005; Geraads and Spassov 2009; Giaourtsakis 2009; Koufos 2016; Koufos et al. 2016; Pandolfi 2018). *Ceratotherium neumayri* (Osborn 1900) has been reported from several fossiliferous localities (MN 10-MN 13) of the Balkan Peninsula, Caucasus, Anatolia and Iran (Osborn 1900; Geraads 1988; Heissig 1999; Geraads and Spassov 2009; Giaourtsakis 2009; Pandolfi 2015). According to Guérin (2011), a taxon closely related with the Balkano-Iranian species *C. neumayri* (*Diceros* cf. *pachygnathus* in Guérin 2011) was present in Africa at Aragai and Ngetabkwony (Kenya, around 6 Ma and 5–4.5 Ma respectively). 'Dihoplus' megarhinus (de Christol 1834) has been recently reported from several latest Miocene (MN 12-MN 13) faunas of Hungary by Pandolfi et al. (2015, 2016), but it was relatively common during the Pliocene (Guérin 1980; Pandolfi et al. 2015, 2016). *Lartetotherium sansaniense* (Lartet in Laurillard, 1848) and 'Dicerorhinus' steinheimensis (Jäger, 1835), first documented during the late early Miocene, also survived during the earliest late Miocene (MN 9) in Europe (Guérin 1980; Heissig 1996, 1999).

The northern African late Miocene localities with remains of Rhinocerotina are relatively scarce and the rhinoceros material was often identified at the generic level (*Ceratotherium* Gray 1868 or *Diceros*, Gray 1821; Geraads 2010: Tab. 34.1). Among the Rhinocerotina species, *Ceratotherium douariense* (= *Diceros douariensis*, Guérin 1966) was established from a partial skull with associated mandible from Douaria (Tunisia, around 7 Ma; Guérin 1980; Geraads 2010). The species was dubitatively recorded at Djebel Krechem (Tunisia, around 10 Ma) by Geraads (1989), mostly on the basis of geographic proximity (Geraads 2010), even though the morphology of the upper teeth is similar to that of *Ceratotherium neumayri* (Geraads 1989, p. 782), from which *C. douariense* is doubtfully distinct according to Geraads (2010). The record of *C. douariense* at Baccinello V3, Italy (Guérin 2000) has been recently discarded (Pandolfi and Rook 2017). A relatively worn P2 collected at Sahabi (Libya, latest Miocene), assigned to *C. neumayri* (= *Diceros neumayri*) by Bernor et al. (1987), has been referred as an undetermined dicerotine by Giaourtsakis et al. (2009) and identified as *C. douariense* by Geraads (2010) and 'Diceros' sp. by Pandolfi and Rook (2019). *Ceratotherium douariense* has also

been reported from the Middle Awash (Ethiopia, latest Miocene; Giaourtsakis et al. 2009), but this record has been re-assigned to *Diceros*? sp. by Geraads (2010: Tab. 34.I) without any detailed discussion.

Ceratotherium? primaevum (= *Dicerorhinus primaevus* Arambourg 1959) was named on a partial juvenile skull and associated remains collected at Bou Hanifia (Algeria, around 10 Ma) by Arambourg (1959). A few isolated remains from the Late Miocene of Chorora (Ethiopia; referred to Dicerotini indet. by Geraads et al. 2002) and of Namurungule Formation (Kenya; referred to *Paradiceros* sp. by Nakaya et al. 1987) could be assigned to *C.? primaevum* (Geraads 2010 and references therein).

cf. *Ceratotherium* sp. was recently reported from the Upper Miocene site of Tizi N'Tadderht (Morocco; Zouhri et al. 2012). Two isolated upper teeth, a fragment of a tooth and an ectocuneiform from Béni Mellal (Morocco, early late Miocene) were assigned to cf. *Paradiceros mukirii* Hooijer, 1968 by Guérin (1976). The latter species was described by Hooijer (1968) on late middle Miocene remains collected at Fort Ternan (Kenya, around 13–14 Ma).

Latest Turolian (MN 13, late Miocene, Messinian) rhinoceroses from central and northern Italy were recently revised by Pandolfi and Rook (2017) and the specimens collected from the localities of Moncucco Torinese (Piedmont), Verduno (Piedmont), Monticino Quarry (Emilia Romagna), and Baccinello V3 (Tuscany) were assigned to 'Dihoplus' megarhinus and Rhinocerotini indet. Only two southern Italian localities, Gravitelli and Cava Gentile, yielded latest Miocene remains of rhinoceros. The specimens collected at Gravitelli (Sicily), assigned to *Rhinoceros* (*Dihoplus*) *schleiermacheri* by Seguenza (1902, 1907), were destroyed during the 1911 Messina earthquake. Hooijer (1946) referred a Dp4 from this locality (Seguenza 1902: Pl.VI, figs 9–11) to ?*Dicerorhinus* sp. and some other bones (assigned as *Hippopotamus* Linnaeus 1758 by Seguenza 1907: Pl. V, figs 51–52; Pl VI, figs 12–13, 21–22) to *Diceros* aff. *pachygnathus* (Wagner 1848). More recently, Guérin (2000) claimed that the material from Gravitelli 'clearly represents *Diceros* but is not sufficient for a determination at the specific level'. According to Pandolfi and Rook (2017), the overall characters of the specimens, deduced from the Seguenza's plates and measurements, suggest an affinity with *C. neumayri*.

Material and methods

Material and morphological comparison

The studied specimen CES CG.R.001 is represented by a partial skull and a fragment of an upper tooth (Figure 3). The specimen was collected in the 1998 by GC and is at present housed at Museo dell'Ambiente, Università del Salento, Lecce (MAUS). The specimen was morphologically compared with the rhinocerotid material collected from several European and African localities (Appendix S1). The comparisons were based on direct observation of the material housed in several museums and institutions, as well as on bibliographic data (Appendix S1). The cranial and dental terminology follows Antoine (2002); the morphometric methodology follows Guérin (1980) with a few additional measurements.

Figure 3. Holotype CES CG.R.001 of *'Ceratotherium' advenientis*, sp. nov., from Cava Gentile, Cessaniti, Italy. (a) Right lateral view; (b) Idem, schematic drawing; (c) Left lateral view; (d) Dorsal view; (e) Basal view; (f) Idem, schematic drawing; (g) Posterior view; (h) Detail of the tooth alveoli, the black arrow indicates the alveolus of P4; (i) Isolated tooth fragment, occlusal view. Scale bar equals 10 cm. a = alveolus; bs = basilar process; cf = condyloid fossa; ch = choanae; fac = posterior alar foramen; fh = frontal horn boss; fm = foramen magnum; fpc = frontal parietal crests; hf = foramen nervi hypoglossi; if = infraorbital foramen; M = molar; mps = mid-palatal suture; nc = nuchal crest; nr = rear border of the nasal notch; nt = nuchal tubercle; oc = occipital condyles; or = orbit; P = premolar; pgp = postglenoidal process; pp = paraoccipital process; pt = pterygoid; tc = temporal condyle; za = zygomatic arch; ptp = posttympanicus process. Grey areas in F indicate the alveoli of molars and premolars.

We collected 69 skulls in lateral view of two extant African dicerotine species (*Diceros bicornis* and *Ceratotherium simum*) and six extinct Rhinocerotidae species (*Ceratotherium neumayri*, *Ceratotherium douariense*, *Diceros gansuensis*, *'Dihoplus' megarhinus*, *Dihoplus pikermiensis* and *Dihoplus schleiermacheri*), which occur in the latest Miocene and early Pliocene fossil record of Western Eurasia and Africa, using both original photos and published pictures. The species list and the number of specimens for each species as well as the list of institutions, where the original specimens are preserved, are reported in Appendix S2. We followed the protocols of Marcus et al. (2000) and Mullin and Taylor (2002) to minimize parallax and measurement error on the photographs.

Cladistic analysis

A cladistic analysis was performed in order to investigate the phylogenetic relationships of the new proposed taxon; 314 characters (70 cranial, 14 mandibular, 130 dental and 100 postcranial) described by Antoine (2002), Antoine et al. (2003), Lu (2013) and Pandolfi (2015) were considered in this work (Appendix S3). All characters are equally weighted, 12 characters are unordered (2, 3, 8, 31, 65, 94, 123, 131, 170, 219, 246, 262) and 302 characters are ordered. The analysis was performed with PAUP 4.0β10 (Swofford 2001), Heuristic search, TBR and 1000 replications with additional random sequence, gaps treated as missing. Thirty eight taxa were included in this analysis (Data Matrix, Appendix S4). The characters states were coded following Antoine (2002), Antoine et al. (2003), Lu (2013), Pandolfi (2015) and direct observations. Among the taxa reported by Lu (2013) and Pandolfi (2015), we retained only the type species within Aceratheriini and we added the following taxa: *Tapirus terrestris* Linnaeus, 1758, *Hyrachyus eximius* Leidy, 1871, *Ceratotherium douariense*, *Diceros gansuensis* Deng and Qiu, 2007, *Paradiceros mukirii* and *Coelodonta antiquitatis* (Blumenbach, 1799). The characters of these taxa were deduced from Arambourg (1959), Guérin (1966, 2011),

Antoine (2002), Antoine et al. (2003), Deng and Qiu (2007), Geraads (2010) and Giaourtsakis et al. (2009), and from direct observations (Appendix S1). The cladistic analysis performed in this paper is mainly based on characters observed on adult individuals that cannot be coded in *C.? primaevum*; accordingly, this taxon is excluded from the analysis to reduce the presence of unstable taxa and polytomies in the tree topologies. The supra-generic classification follows Antoine (2003).

Geometric morphometrics

Geometric morphometrics represents a useful tool to quantify shape changes and phenotypic differences among taxa (Adams et al. 2004; Zelditch et al. 2012). Sixteen landmarks and 9 semilandmarks in two dimensions (Figure 4) were digitized on each skull in lateral view, using tpsDig2 v2.17 (Rohlf 2013). Scale bars were used to scale each digitized specimen. Semilandmarks are useful to capture morphological information of outlines where no homologous points can be detected. Curves or contours are assumed to be homologous among specimens (Bookstein et al. 2002; Pérez et al. 2006). We digitized semilandmarks at equal distance along outlines drawn on the specimens. We excluded from the landmark configuration the nasal and premaxillary bones, which are not preserved in CES CG.R.001 and are badly preserved in some skulls considered for comparison. Generalized Procrustes Analysis (GPA, Bookstein 1991), performed using the procSym() function in 'Morpho' R package (Schlager 2013), was used to analyze shape among specimens in the cranial samples. Generalized Procrustes analysis scales, aligns, and rotates each landmark configuration to the unit centroid size (i.e., the square root of sum of squared differences between landmarks from their centroid;

Bookstein 1986). After GPA, a Principal Components Analysis (PCA) was performed on the Procrustes shape variables to identify orthogonal axes of maximal variation in the dataset.

UPGMA

A cluster analysis was performed on cranial shape data to assess morphological similarities among taxa included in the dataset. Procrustes distances were agglomerated by means of a UPGMA (Unweighted Pair Group Method with Arithmetic mean) algorithm.

Institutional abbreviations

AMNH, American Museum of Natural History, New York, USA; **BSPG**, Bayerische Staatssammlung für Paläontologie und Geologie, Munich, Germany; **HNHM**, Hungarian Natural History Museum, Budapest, Hungary; **IGF**, Museo di Storia Naturale, sezione di Geologia e Paleontologia, Florence, Italy; **IRSNB**, Institut royal des Sciences naturelles de Belgique, Bruxelles, Belgium; **IVPP**, Institute of Vertebrate Paleontology and Paleoanthropology, Chinese Academy of Sciences, Beijing, China; **MAC**, Museo di Anatomia Comparata, Sapienza Università di Roma, Rome, Italy; **MAUS**, Museo dell'Ambiente, Università del Salento, Lecce, Italy; **MFGI**, Geological and Geophysical Institute of Hungary, Budapest, Hungary; **MfN**, Museum für Naturkunde, Berlin, Germany; **MGGC**, Museo di Geologia Giovanni Capellini, Bologna, Italy; **MNCN**, Museo Nacional de Ciencias Naturales, Madrid, Spain; **MNHNP**, Muséum national d'Histoire naturelle, Paris, France; **MPP**, Museo di Paleontologia, Università di Parma, Parma, Italy; **MPPB**, Museo di Palazzo Poggi, Bologna, Italy; **MSNAF**, Museo di Storia Naturale, Accademia dei Fisiocritici, Siena, Italy; **MSNF**, Museo di Storia Naturale, sezione di Zoologia, Florence, Italy; **NHMUK**, Natural History Museum, London, United Kingdom; **NHMW**, Naturhistorisches Museum, Wien, Austria; **NMB**, Naturhistorisches Museum, Basel, Switzerland; **SMF**, Senckenberg Naturmuseum, Frankfurt, Germany; **ZSM**, Zoologische Staatssammlung, Munich, Germany.
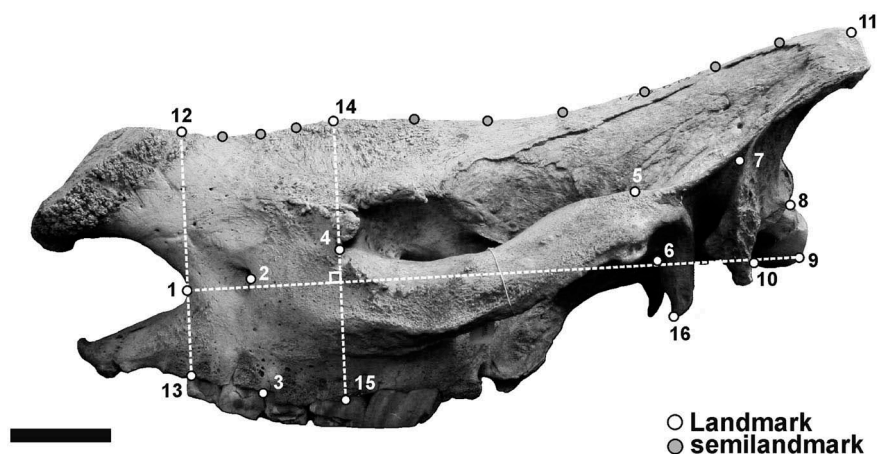

Figure 4. Landmark and semilandmark configuration of skull in lateral view (*Ceratotherium simum*, NHMUK 1963-8-13-2): (1) posterior border of the nasal notch; (2) infraorbital foramen; (3) posterior border of the upper premolar row; (4) anterior border of the orbit; (5) dorsal tip of the zygomatic arch; (6) ventral concavity of the posterior part of the zygomatic arch; (7) dorsal tip of the auditory pseudomeatus; (8) dorsal tip of the occipital condyle; (9) posterior tip of the occipital condyle; (10) ventral tip of the occipital condyle; (11) maximum curvature point of the posterior area of the occipital crest; (12) projection of the landmark #1 on the dorsal border of the nasal bones; (13) projection of the landmark #1 on the ventral border of the premaxillary bones; (14) projection of the landmark #5 on the dorsal border of the frontal bones; (15) projection of the landmark #5 on the ventral border of the maxillary bones; (16) ventral tip of the processus postglenoidalis. Scale bar equals 10 cm.

Other abbreviations

ch. = character; Dp = upper deciduous cheek tooth; dp = lower deciduous cheek tooth; I = upper incisor; i = lower incisor; L = length; M = upper molar; m = lower molar; MC = metacarpal; mm = millimetres; ca = *circa* (about); MN = Mammal Neogene Zones; MT = metatarsal; P = upper premolar; p = lower premolar; Wa = anterior width; Wp = posterior width.

Systematic palaeontology

Order **Perissodactyla** Owen, 1848
Family **Rhinocerotidae** Gray, 1821
Tribe **Rhinocerotini** Gray, 1821
Subtribe **Rhinocerotina** Gray, 1821
Genus ***Ceratotherium***

'Ceratotherium' **advenientis**, sp. nov. (Figure 3)

Derivation of the name. From the genitive of participle of the Latin *adveniēns*, which means arriving, in reference to the movement of the Calabro-Peloritan arc, which was part of the African continent during the late Miocene.

Type specimen. CES CG.R.001, skull lacking parts of the zygomatic arches, the tooth rows, the premaxillae and the rostral part of the nasal bones (Figure 3).

Diagnosis. Two-horned large-sized rhinoceros, *'Ceratotherium' advenientis* can be diagnosed by two autapomorphies: (1) concave dorsal profile of the skull and (2) concave occipital crest. The skull is slightly concave in lateral view, the occipital face is vertical. The occipital face, in posterior view, is very wide and laterally expanded, almost semi-circular in outline; the foramen magnum is sub-circular. The nuchal crest is wider than in the extant African rhinoceroses, *C. neumayri*, *C. douariense*, and European latest Miocene species. Differs from *Paradiceros mukirii* in the following features: (1) vertical occipital face; (2) frontal horn boss little developed and more anteriorly placed; and (3) longer distance between the rear border of the nasal notch and the anterior border of the orbit. Differs from *Diceros bicornis* in having a wider nuchal crest, a less concave dorsal profile of the skull, and a partially closed external auditory pseudo-meatus. Differs from *Ceratotherium simum* in having a wider nuchal crest, a laterally larger occipital face in posterior view, and a vertical occipital face in lateral view.

Occurrence. base of Unit CG. SH2 at Cava Gentile, Cessaniti, Vibo Valentia, Southern Italy, late Miocene, between 8.2 and 7.1 Ma (Marra et al. 2017).

Description

Skull. In lateral view (Figure 3(a–c)), the dorsal profile of the skull is slightly concave, the frontal horn boss is evident, the processus postorbitalis is absent, the external auditory pseudo-meatus is partially opened ventrally, the area between the temporal and nuchal crest is depressed and the occipital face is vertical (Figure 3(a–c)); the nuchal tubercle is well-developed,

the frontal-parietal crests are evident; the infraorbital foramen is placed behind the nasal notch, and the foramen sphenorbitale and foramen rotundum are fused. In dorsal view (Figure 3(d)), CES CG.R.001 displays a little-developed frontal horn boss, close frontal-parietal crests, and a concave posterior border of the nuchal crest (Figure 3(d)). A rugosity for the nasal horn is visible on the preserved part of nasal bones. In ventral view (Figure 3(e,f)), at the level of the infraorbital foramen, the alveoli for four roots of a rectangular-shaped tooth (wider than long; Figure 3(h)), a P4, are evident; remnants of a larger tooth (M1) are located rear to the previous one. The lingual border of the alveoli for two other teeth (M2, at the level of the anterior border of the orbit, and M3) can be detected. Thus, the rear border of the nasal notch is at the level of P3, the infraorbital foramen is at the level of P4, and the anterior border of the orbit is at the level of M2. The anterior border of the choanae is rather convex, the palatine spine and the vomer are not visible. The pterygoids are rather damaged but their posterior margin is nearly horizontal. The morphology of the lacerate, oval, and spinous foramina is not visible, because that area is filled by an encrusted sediment; the processus postglenoidalis is well developed and, in ventral view, the main axis of its cross section is oblique in respect to the long axis of the skull and displays a convex antero-lateral border; the postero-lateral border is narrower than the antero-lateral one. The basilar process has a sagittal crest, the foramen nervi hypoglossi is placed in the middle of the condyloid fossa. In posterior view (Figure 3(g)), the occipital face is wide, the nuchal crest is relatively well developed, and its dorsal profile is concave; the foramen magnum is circular and the dorsal incision is absent. The premaxillae and the teeth are missing, though the tooth roots are partially preserved.

Tooth. A fragment of a right triangular M3 (Figure 3(i)) was collected together with the skull. In occlusal view, this tooth displays a small crochet, a lingually open median valley, and a mesial cingulum. The enamel is poorly preserved, but it is thin and rough.

Geometric morphometrics

Cranial shape variation. The first 12 principal components of the bgPCA, performed on the skulls, in lateral view, explain collectively 95% of total shape variance. Figure 5(a) shows the relationship between PC1 (42.08% of the total shape variance explained) and PC2 (14.97% of the total shape variance). In Figure 5(b), we report the plot between PC1 and PC3 (the latter corresponding to 11.89% of the total shape variation). Negative PC1 values are associated with a short skull having a short upper tooth row, short occipital crest, a strongly concave dorsal profile, and an anterior border of the orbit close to the posterior end of the nasal notch. This cranial morphology is *Diceros*-like. Positive PC1 values are associated with a long skull, having a long upper tooth row, a long occipital crest, a slightly concave dorsal profile, and an anterior border of the orbit less close to the nasal notch. This morphological arrangement is *Ceratotherium*-like.

At positive PC2 values the skull is long, having a slightly dorsal concave profile, the orbit pretty close to the nasal notch, a moderately long occipital crest and a long upper tooth row, whereas at negative PC2 values the skull is
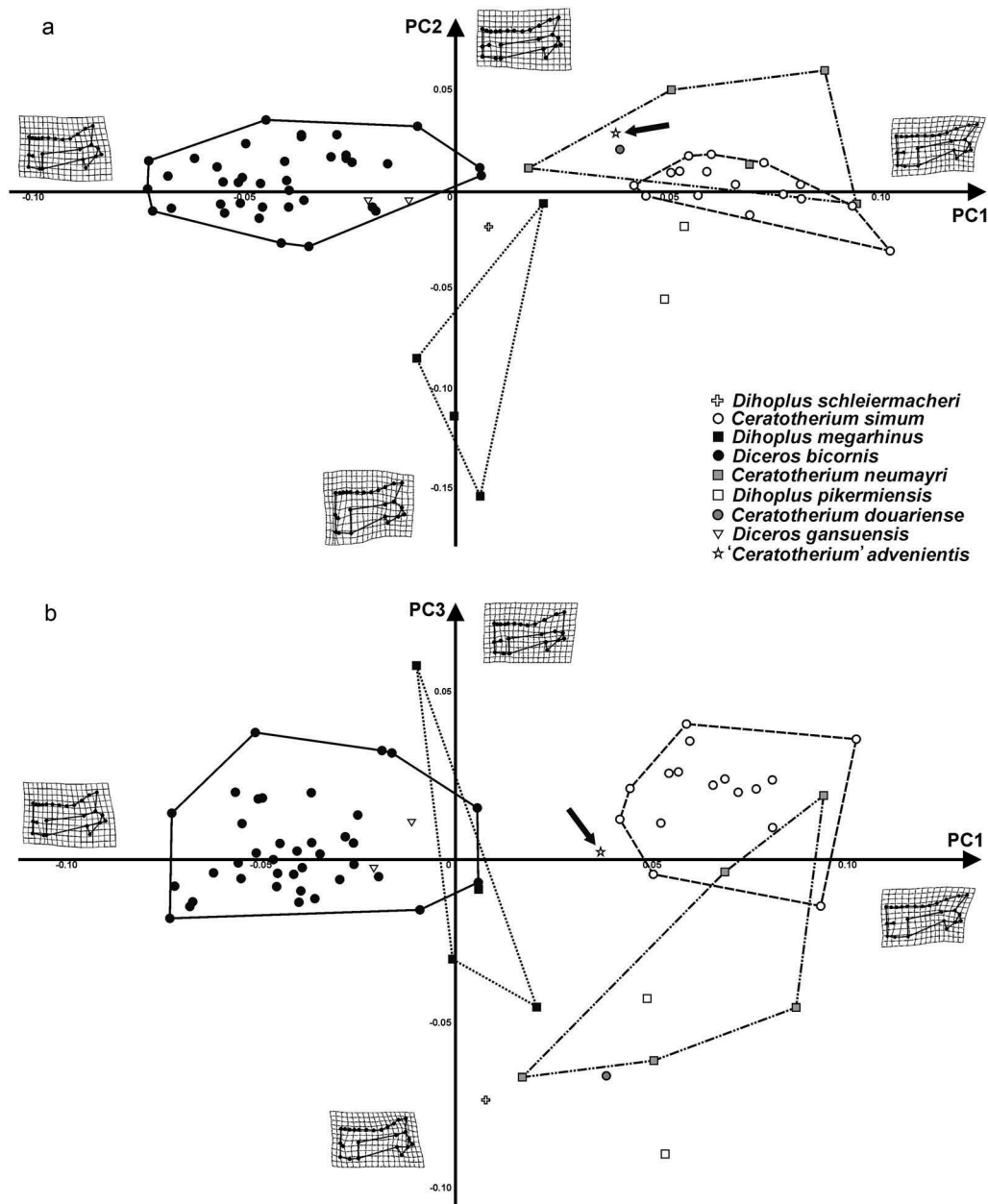
Figure 5. Principal component analysis performed on the compared skulls in lateral view. (a) Relationship between PC1 and PC2; (b) Relationship between PC1 and PC3. The black arrow indicates the position of *'Ceratotherium' advenientis* sp. nov. in the morphospace.

massive, slightly shorter, having a dorsal concave profile, an orbit less close to the nasal notch, and a moderately long occipital crest.

The skull is high and has a moderate concave profile, and an anterior border of the orbit close to the nasal notch at positive PC3 values (Figure 5(b)). A skull having a concave dorsal profile, a orbit distant from the nasal notch is typical of negative PC3 values.

In summary, the extant *Diceros bicornis* is located at negative PC1 values along with *D. gansuensis*, whereas the extant *Ceratotherium simum* occurs at positive PC1 values together with *Ceratotherium neumayri* and *Dihoplus pikermiensis*. *'Dihoplus' megarhinus* and *D. schleiermacheri* lie at negative PC2 values. *Ceratotherium douariense* falls within the morphospace of *C. neumayri*, at positive PC1 and PC2 values and

negative PC3 values. *'Ceratotherium' advenientis* lies between *C. simum* and *C. neumayri* at positive PC1 and PC2 values.

Cluster analysis. In the UPGMA dendrogram of averaged cranial shape similarities (Figure 6), *'Ceratotherium' advenientis* clusters with the grazer *C. simum* and the mixed feeder *C. neumayri*. *Diceros bicornis* clusters with *D. gansuensis* and *C. douariense* with *D. pikermiensis*, indicating similar morphology between each other.

Phylogenetic analysis

A cladistic analysis was performed here in order to investigate the phylogenetic relationships of the Cava Gentile rhinoceros and to support its taxonomic position.
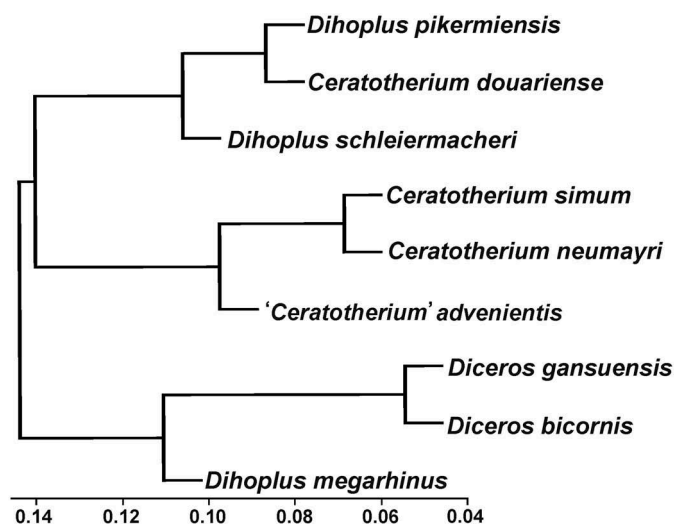
Figure 6. UPGMA cluster analysis performed on compared skulls in lateral view.

The analysis based on 39 taxa and 314 characters produced one most parsimonious tree, reported in Figure 7 (Tree Length = 1547 steps, Consistency Index = 0.259, Retention Index = 0.51; Homoplasy Index = 0.74).

Rhinocerotinae (node A), as previously defined by Antoine et al. (2010), is represented by Rhinocerotinae *incertae sedis* (aceratheres *sensu latu*) and two tribes: Aceratheriini and Rhinocerotini. In the present analysis, the topology of the obtained tree resembles in several aspects that reported by Antoine et al. (2010) and is similar to that published by Lu et al. (2016). Similarly to the results published by Lu et al. (2016), Aceratheriini results as a polyphyletic group, with a major clade composed by the genera *Persiatherium, Acerorhinus, Chilotherium, Shansirhinus, Plesiaceratherium* and *Subchilotherium* (node B) and a minor clade composed by *Alicornops, Aceratherium* and *Hoploaceratherium* (node C); the latter resulting as sister group of Rhinocerotini (node D). The relationship between node C and node D, node E, is here supported by eight unambiguous synapomorphies: long metaloph on M1-2 (ch. 151[0]), straight posterior part of ectoloph on M1-2 (ch. 152[0]), hypocone isolated on M1 (ch. 155[1]), lingual cingulum usually absent on lower premolars (ch. 179[2]), lingual cingulum usually absent on lower molars (ch. 189[2]), pyramidal-facet and McV-facet always in contact on the unciform (ch. 254[2]), straight magnum-facet on McII (ch. 256[1]), posterior McIII-facet always present on McII (ch. 258[2]). Among these characters, ch. 152, 179, 189, 256 and relative states were also detected by Lu et al. (2016) for the same node. In agreement with Lu et al. (2016) further investigation are needed to clarify the relationships among and within aceratheriines.

The Rhinocerotini clade (node D) is here supported by nine unambiguous synapomorphies: concave dorsal profile of the skull (ch. 25[1]), distant frontal-parietal crests (ch. 49[2]), wide transverse expansion of the occipital crest (ch. 50[1]), nearly horizontal symphysis (ch. 71[2]), paralophid nearly reaches the lingual rim on the lower teeth (ch.172[0]), U-shaped occlusal outline of trigonid basin on the lower teeth (ch. 173[0]), absence of lingual cingulum on the lower premolars (ch. 179[3]), absence of ectolophid fold on dp2-dp3 (ch. 209[1]) and rounded posterior apophysis on the tibia (ch. 279[1]). The first dichotomy within Rhinocerotini isolates the clade Teleoceratina (node F) and the clade Rhinocerotina (node G).

Rhinocerotina is here supported by 16 unambiguous synapomorphies: nasal notch above P1-P3 (ch. 7[0]), broad rostral end of the nasal bones (ch. 38[1]), nasal bones anteriorly separated (ch. 39[1]), presence of a frontal nasal horn (ch. 41[1]), protocone constricted just anteriorly on the upper teeth (ch. 108[1]), absence of labial cingulum on the upper premolars (ch. 112[3]), lingual cingulum on P2-P4 usually present (ch. 116[1]), reduced lingual cingulum on P2-P4 (ch. 117[1]), absence of labial cingulum on the upper molars (ch. 138[3]), absence of antecrochet on the upper molars (ch. 139[0]), absence of labial cingulum on the lower premolars (ch. 181[1]), curved paralophid on p2 (ch. 186[1]), labial cingulum usually absent on the lower molars (ch. 191[2]), triangular outline of the proximal facet on MCIV (ch. 262[2]), facets 2 and 3 for the calcaneus usually fused on the astragalus (ch. 295[2]), intermediate relief low and smooth on the metapodials (ch. 312[1]). Characters 7, 38, 39, 41, 108, 112, 116, 138, 139, 181, 186 and 191 have been also recognised by Lu (2013) to support this clade. Characters 38, 41, 138 and 139 have been also diagnosed by Antoine et al. (2010) for Rhinocerotina.

Within Rhinocerotina, the first dichotomy (node H) isolates the (*Gaindatherium browni, Lartetotherium sansaniense*) clade and the second dichotomy (node I) isolates the *Rhinoceros* clade (*R. unicornis, R. sondaicus*). The latter group is here supported by eight unambiguous synapomorphies: ventrally closed external auditory pseudo-meatus (ch. 28[2]), (ch. 34[1]), zygomatic width/frontal width ratio >1.5 (ch. 48[1]), trapezoidal shaped occipital face (ch. 65[1]), vertical ramus of the mandible inclined forward (ch. 82[1]), proximal ulna-facets always fused on the radius (231[3]), indentation on the medial side of the magnum absent (250[0]), distal widening of diaphysis present on MTIII (306[1]). The third dichotomy (node L) isolates a clade of the two-horned rhinoceros and this node is supported by 11 unambiguous synapomorphies: rough suture jugal/squamosal (ch. 24[1]), dolichocephalic skull (ch. 35[0]), presence of frontal horn (ch. 45[1]), very upraised symphysis (ch. 71[1]), absence of lingual groove on the corpus mandibulae (ch. 78[1]), presence of mesostyle on M2 (ch. 160[1]), transversally concave axis-facets on the atlas (ch. 219[2]), L-shaped distal facet for semilunate on pyramidal (246[2]), pyramidal-facet and MCV-facet always separated on the unciform (ch. 254[0]), trapezium-facet always absent on MCII (ch. 260[2]), flat insertion of muscle *extensor carpalis* on metacarpals (ch. 264[0]), low trochanter major on the femur (ch. 266[1]). The node M includes two clades. One of them (node N) with the species of the genus *Dihoplus* and the other one (node O) with the extant African rhinoceroses, their relatives, and *Coelodonta antiquitatis*. The new taxon, '*Ceratotherium*' *advenientis*, is included within this latter clade (Figure 7).

The clade composed by the two species of the genus *Dihoplus* (*D. schleiermacheri* and *D. pikermiensis*; node N) is supported by 11 unambiguous synapomorphies: undulated dorsal profile of the nasal bones (ch. 2[1]), U-shaped nasal notch (ch. 8[0]),
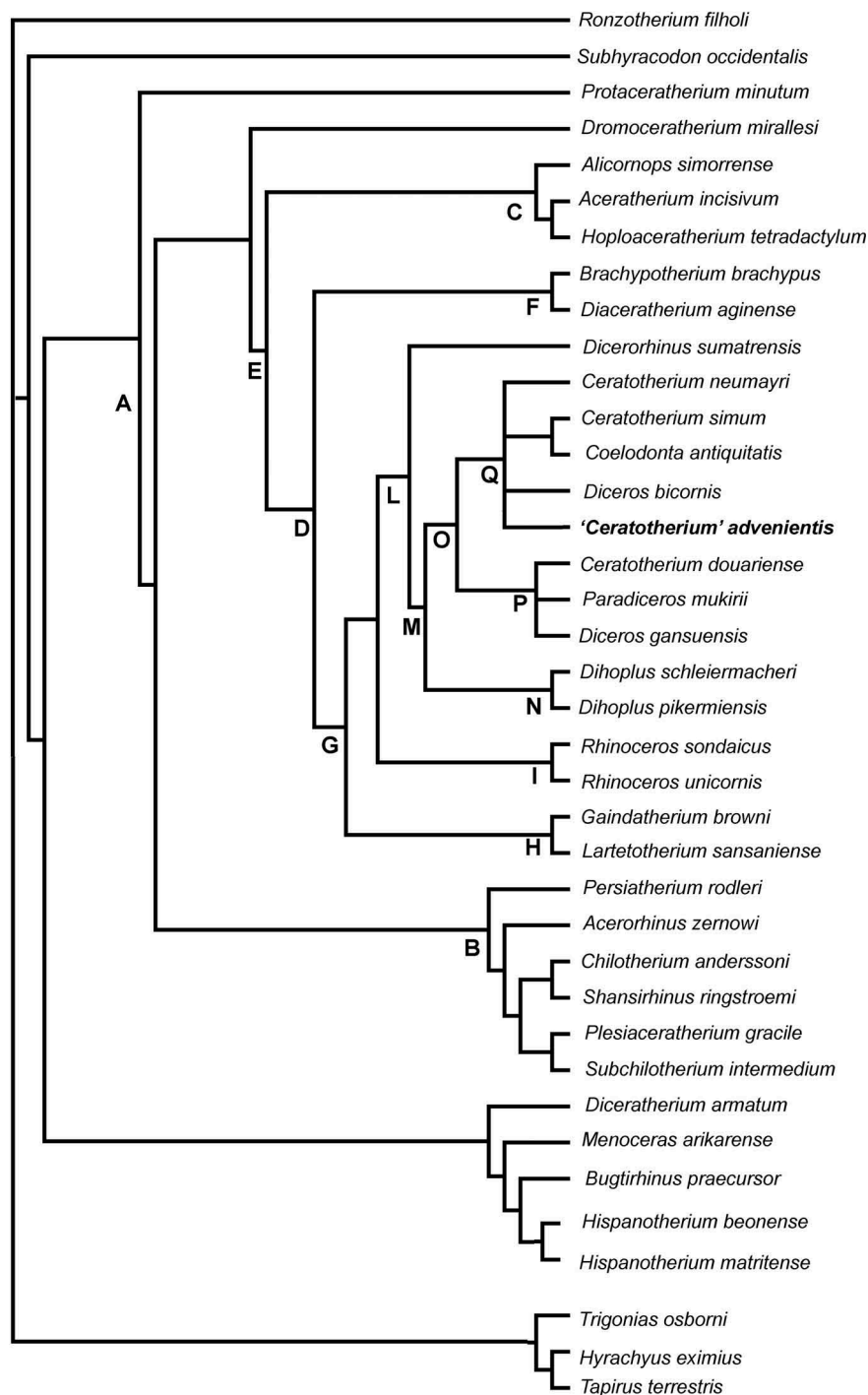
Figure 7. The strict consensus tree of the phylogenetic relationships of *'Ceratotherium' advenientis* sp. nov. within Rhinocerotidae. A–Q refer to nodes discussed in the text.

presence of processus postorbitalis (22[0]), abrupt narrowing of the dorsal surface of the skull, anterior to orbit (36[1]), nasal bones fused (39[2]), straight transversal profile of the articular tubercle on the squamosal (ch. 56[0]), absence of cement on the cheek teeth (87[0]), lingual bridge between protocone and hypocone on P2 (123[1]), hypocone anterior to the metacone on P2 (ch. 124[1]), crista usually present on P3 (ch. 134[2]) and protocone constriction usually absent on M3 (165[1]). The node O is here supported by 11 unambiguous synapomorphies: very concave dorsal profile of the skull (ch. 25[2]), very broad rostral end of the nasal bones (ch. 38[2]), presence of lateral projection

of the orbit (ch. 47[1]), absence of median ridge on the condyles (ch. 68[0]), very upraised symphysis on the mandible (ch. 71[0]), convex base of the corpus mandibulae (ch. 80[1]), well developed processus coronoideus on the mandible (ch. 83[0]), absence of I1 (ch. 93[1]), absence of i2 (ch. 100[1]), protocone constriction always absent on M1-M2 (ch. 145[1]) and absence of mesostyle on DP2 (ch. 197[1]).

The clade composed by *C. douariense, P. mukirii* and *D. gansuensis* (node P) is supported only by five unambiguous synapomorphies: brachycephalic skull (ch. 35[1]), abundant cement on cheekteeth (ch. 88[1]), lingual cingulum always

present on P2-P4 (ch. 116[0]), crista always absent on the upper molars (ch. 142[0]) and reduced paraconid on p2 (ch. 187[1]).

The node Q includes a polytomy with *D. bicornis, C. neumayri*, the new taxon and a small clade composed by *Ceratotheirum simum* and *Coelodonta antiquitatis*. It is supported by eight unambiguous synapomorphies: presence of constriction of ventral edge anterior to temporal condyle (ch. 20[0]), prominent dorsal surface of parietal crest (ch. 51[1]), very convex base of corpus mandibulae (ch. 80[2]), vertical ramus of the mandible inclined backward (ch. 82[2]), foramen mandibulare above the teeth neck (ch. 84[1]) and antecrochet usually absent on the upper molars (ch. 139[1]), V-shaped occlusal outline of the trigonid basin (ch. 173[1]).

In the present analysis, 'Ceratotherium' advenientis is defined by two autapomorphies: concave dorsal profile of the skull (ch. 25[1]) and concave occipital crest (ch. 52[0]).

Discussion

Comparative remarks

Comparison with elasmotheres
The late Miocene species belonging to Elasmotherinae (e.g., *Parelasmotherium; Ninxiatherium; Iranotherium*) differ from 'Ceratotherium' advenientis in having longer skull usually with a backwardly extended nuchal crest, and absence of insertion for the frontal horn (*Parelasmotherium; Ninxiatherium; Iranotherium*) or nasal horn (*Sinotherium*) (Antoine 2002; Deng 2007, 2008).

Comparison with Eurasian and African Aceratheriini
Aceratheres lack the insertion for the frontal horn and, with a few exceptions, also for the nasal horn (Heissig 1999; Pandolfi 2015). The skull is smaller, less massive and shorter than that of 'Ceratotherium' advenientis, with a less-developed nuchal crest and usually a trapezoidal occipital face.

Comparison with Eurasian and African Teleoceratina
The skull of the species belonging to this group (Heissig 1999) is shorter and lacks the insertion for the frontal horn. The nasals are narrow, the occipital face is smaller and proportionally narrower than in the studied specimen, with a less developed nuchal crest.

Comparison with extant African rhinoceroses
Compared with *D. bicornis* (Appendix S1), the Cava Gentile's skull displays a less concave dorsal profile, a wider nuchal crest, a larger occipital face, a smaller frontal boss, and a partially ventrally closed external auditory pseudo-meatus (Figures S1, S2). The skull of *C. simum* (Appendix S1) displays a backwardly extended nuchal crest, an inclined backward occipital face, a larger insertion for the frontal horn, the tooth row more anteriorly placed, and a quadrangular M3 with thick enamel and complex folding (Figures S1, S2).

Comparison with latest Miocene Rhinocerotina
The skulls of *Ceratotherium neumayri* (Figure S1) display a much more backwardly extended nuchal crest in lateral

view, a forked nuchal crest in dorsal view, an inclined backward occipital face in lateral view and the posterior border of the nasal notch between P2 and P3 (Figure S1, cfr. Geraads 2005; Appendix S1). The occipital face is narrower and dimensionally smaller (including the occipital condyles) in respect to the Cava Gentile skull (Table 1).

Ceratotherium douariense from Douaria has the posterior border of the nasal notch, at the level of the anterior border of P3, and the posterior border of the infraorbital foramen, at the level of P3-P4 transition, more anteriorly placed in respect to CES CG.R.001 (cfr. Geraads 2005). The processus postglenoidalis is less massive and less developed antero-posteriorly than in the Cava Gentile's skull; the dorsal border of the nasals, at the level of the posterior border of the nasal notch, is more inclined upwards in *C. douariense* (Figure S1). In the latter taxon, the distance between the orbit and the posterior border of the nasal notch is shorter than in CES CG.R.001 (Table 1). The skull from the Middle Awash referred to *Diceros douariensis* by Giaourtsakis et al. (2009) and reported as *Diceros*? sp. by Geraads (2010: Tab. 34.I) has an open external auditory pseudo-meatus (Giaourtsakis et al. 2009: Fig. 14.1), the dorsal profile of the skull in lateral view is more concave than in the studied specimen, the distance between the frontal-parietal crests is wider, the occipital face is less developed and the nuchal crest is less wide than in the specimen from Cava Gentile (Figure S1).

The skull from Cava Gentile is larger than that of *Paradiceros mukirii* (Hooijer 1968; Geraads 2010: Fig. 34.5; Guérin 2011: Figure 4(b), Figure 5; Table 1) and it morphologically differs from the latter in having a more vertical occipital face, a frontal boss little developed and more anteriorly placed, and a longer distance between the rear border of the nasal notch and the anterior border of the orbit.

In respect to the Chinese *Diceros gansuensis* (Deng and Qiu 2007: Figure 1), the Cava Gentile skull has a wider nuchal crest, a larger occipital face, and a less concave dorsal profile of the skull. The occipital face in *D. gansuensis* (Deng and Qiu 2007: Figure 4(c)) is trapezoidal and proportionally higher than in the studied specimen. The external auditory pseudo-meatus is partially closed in *D. gansuensis* as well as in the specimen from Cava Gentile and *C. neumayri*.

Ceratotherium? primaevum is poorly known and the cranial features described by Arambourg (1959) are based on a juvenile skull lacking the occipital portion. The specimen was firstly assigned to *Dicerorhinus*, but Geraads (1986) suggested an attribution to Dicerotini indet. and Geraads (2010) provisionally included it in the paraphyletic genus *Ceratotherium*. The juvenile skull has strong nasal and frontal horn bosses, lacks the postorbital process on the frontal, displays a well-developed supraorbital process and the ventral border of the orbit is laterally inclined. In respect to 'Ceratotherium' advenientis, the infraorbital foramen is more posteriorly placed; the ratio between the distance between the infraorbital foramen and the rear border of the nasal notch and between the latter point and the orbit is higher (ca 0.318 versus ca 0.15 in 'Ceratotherium' advenientis). A comparison with several skulls of *D. bicornis* at different ontogenetic stage revealed that this ratio is approximately constant, varying from 0.25 to 0.3 in the black rhinoceros (Appendix S5).

Table 1. Measurements (in mm) of the skull CES CG.R.001 of *'Ceratotherium' advenientis* sp. nov. from Cava Gentile (Italy), compared with *Paradiceros mukirii* (data from Guérin 2011), *C. douariense* (data from Guérin 1966; Giaourtsakis et al. 2009), *Ceratotherium? primaevum* (data from Arambourg 1959), *Diceros praecox* (data from Hooijer and Patterson 1972), *Ceratotherium neumayri* (data from Geraads 1988; Antoine and Saraç 2005; Geraads and Spassov 2009; Giaourtsakis 2009; Antoine et al. 2012), *Dihoplus pikermiensis* (data from Geraads 1988; Geraads and Spassov 2009), *'Dihoplus' megarhinus* from several Pliocene localities of Western Europe (from Guérin 1980), *Dihoplus schleiermacheri* (Late Miocene, Central Europe: Guérin 1980), *Ceratotherium simum* (data from Guérin 1980), and *Diceros bicornis* (data from Guérin 1980). *estimated from published pictures; (1) based on the specimens NHMUK49660, M10142, M10141; (2) based on the specimen NHMUKM2781.

Measurement	N° in Guérin 1980	Ceratotherium' advenientis	Paradiceros mukirii	Ceratotherium douariensis	Ceratotherium? primaevum	Diceros praecox	Ceratotherium neumayri	Dihoplus pikermiensis	Dihoplus mega- rhinus W.E. Pliocene	Dihoplus schleiermacheri	Ceratotherium simum	Diceros bicornis
Maximal length from nasal boss to nuchal crest	3						ca 560–740	620–700	690–808	679	667–836	480–655
Width of dorsal edge nuchal crest	15	276.84		ca 208			ca 190–235	ca 150–215	165- ca 211	144–175	181.5–249	114.5–211
Maximum width of the occiput	16	288.97	est. 160				ca 150–240	210–275	243–282	289.71[2]	212–291	191–263.5
Distance between the frontalparietal crests	17	43.34		68–78		80	53–61	ca 30.45[1]	43.5-(70)	0	230.5–307	30.5–101
Maximum width of cranium at orbits	20	(259)				355	(250)	ca 172[1]	210–264	246.70[2]	232–328	211–312
Height of the occipital face from the top of foramen magnum to nuchal crest	23	160.58					143- ca 160	142–155	167–190	145–182	149–185	130–180
Foramen magnum width	31	57.84					36–46	37.47[1]	72	51.71[2]	50–65.5	42–67
Width of occipital condyles	32	157.33					124–130	128.83[1]	127–158	135.62[2]	133–172.5	112–150
Height of the occipital face from the base of foramen magnum to nuchal crest		214.64					220	ca 201–210.44[1]	220	225.58[2]		
Transverse diameter of the postorbital constriction	5	116.74	est. 105					ca 74[1]		20.84[2]	94–121	96–147
Transverse diameter of the frontal bones		(212)										
Length from the infraorbital foramento the nasal notch		22.35			35							
Length from the orbital cavity to the infraorbital foramen		105.98										
Length from the orbital cavity to the nasal notch	9	140	102	128*	110			138.79–142.90[1]		161.95[2]	160–198	104–156.5
Length from the orbital cavity to the nuchal crest	8	354.36				ca 440		360–377[1]		336[2]	395–515	325–424
Length from the nuchal crest to the postorbital apophysis	6	315.55						285.9–293.64[1]		259.28[2]		
Length from the occipital condyles to the formen palatale		363.48										
Length from the foramen magnum to the foramen palatale		340.69						301.52[1]				

The material from Cava Gentile differs from *Dihoplus schleiermacheri*, in which the frontal-parietal crests are very close to each other, the posterior border of the nuchal crest is straight and transversally less developed, and the posterior border of the nasal notch is at the level of P2 (Figure S1).

The dorsal profile of the skull is concave in the specimen NHML M49660 ascribed to *Dihoplus pikermiensis* (Geraads 1988; Giaourtsakis et al. 2006). Nevertheless, this feature could be overestimated by a lateral deformation of the skull. Other specimens collected at Pikermi and housed at NHML do not display such a markedly concave profile of the skull (Figure S1). In this species, the posterior border of the nasal notch generally reaches the level of P2-P3, and the frontal-parietal crests are relatively closer (except for the specimen NHMW 2009z-0085-0001 which is dorso-ventrally compressed). The skulls of *D. pikermiensis* display a trapezoidal occipital face (Figure S2) and the nuchal crest is less developed than in the skull from Cava Gentile. In addition, in *D. pikermiensis* the foramen magnum is subtriangular, and, in lateral view, the rear borders of the zygomatic arches are much more elevated than in the studied specimen.

In the skull of '*Dihoplus*' *megarhinus* (Appendix S1), the dorsal profile is more concave between the parietal and the frontal bones in respect to the studied specimen, the external auditory pseudo-meatus is fully closed, the frontal-parietal crests are distant, the insertion for the frontal horn is wider and more marked, and the occipital face is trapezoidal in posterior view.

The morphology of the skull CES CG.R.001 allows to include it within the subtribe Rhinocerotina; however, the studied specimen clearly differs from the known late Miocene European rhinocerotines. The shape analysis, in lateral view only and considering the available configuration, placed CES CG.R.001 close to *Ceratotherium*, whereas the cladistic analysis placed it in a clade composed by *D. bicornis, C. neumayri* and *C. simum+C. antiquitatis*. The skull CES CG.R.001 resembles the genus *Diceros* for a few characters, in particular in the development of the occipital face (wider than high) and its rather vertical position (Figure S2), in the low position of the rear border of the zygomatic arch and in the enlargement of the postglenoidal process. An inclusion into the genus *Diceros* of the studied skull can be excluded due to the peculiar morphological features of CES CG.R.001. Accordingly, due to the result obtained by UPGMA analysis and the unresolved position in the cladistic analysis, the new species from Cava Gentile is provisionally assigned to the genus *Ceratotherium* pending the discovery of much more cranial material.

Considerations on the cranial shape

When exploring the cranial morphology in lateral view, '*Ceratotherium*' *adventientis* appears separated from *Diceros bicornis* in the cranial morphospace (Figure 5), located in an intermediate position between the black extant rhinoceros and the white extant rhinoceros. '*Ceratotherium*' *adventientis* is close to *C. simum* and *C. neumayri* at positive PC1 and PC2 values but would appear morphologically distant from *C. neumayri* and *C. douariense* at negative PC3 values. The

cluster analysis confirms that '*Ceratotherium*' *adventientis* is morphologically similar to *C. simum* and *C. neumayri* for the considered configuration.

Unfortunately, it is impossible to investigate if any significant morphological differences of '*Ceratotherium*' *adventientis* occur with other species using a multivariate analysis of variance due to the presence of a single skull in the dataset belonging to this new taxon. Those results, however, support '*Ceratotherium*' *adventientis* as a different taxon with respect to *Diceros* and *Ceratotherium*, having a cranial shape, in lateral view, intermediate between the two genera.

Phylogenetic considerations

The consensus topology is similar to that obtained by Antoine et al. (2010) and Lu et al. (2016) concerning the relationships within the considered taxa.

The monophyly of elasmotheres has been supported and discussed in several papers (Antoine 2002; Antoine et al. 2003). The polyphyly of Aceratheriini has been also detected by Lu et al. (2016). Considering the extant species, a tree topology similar to that obtained by the present analysis was reported by Antoine et al. (2003, 2010); the phylogenetic relationships within the extant species (Figure 7) supports the phylogenetic hypothesis of the number of horns proposed by Simpson (1945) and Loose (1975), indicating the presence of one horn as an ancestral condition within the extant species, and supporting the monophyletic origin of two-horned rhinoceroses (African and Sumatran rhinos).

The position of '*Ceratotherium*' *adventientis* might be affected by the lack of dental data; however, the cranial shape change is much more phylogenetically constrained (Piras et al. 2010; Pandolfi and Maiorino 2016) than changes in tooth morphologies, which have been driven more by adaptation than by shared ancestry (Piras et al. 2010; Raia et al. 2010; Pandolfi and Maiorino 2016). The absence of processus postorbitalis on the frontal bone and the development of the nuchal tubercle suggest an affinity with the African species. The morphological features and proportions of the neurocranial portion of '*Ceratotherium*' *adventientis* suggest a morphologically affinity with *D. bicornis*, despite the shape analysis in lateral view suggested a closeness to *Ceratotherium*.

The phylogenetic relationships of *Paradiceros mukirii* were mainly based on morphological studies. The cladistic analysis performed by Cerdeño (1995: fig. 2) showed *Paradiceros* as sister taxon of the (*Diceros, Ceratotherium*) clade. Accordingly, *Paradiceros* has been usually considered as a primitive dicerotine, but Geraads (2010) recently raised some issues concerning the relationship of this taxon with dicerotines in particular on the basis of the peculiar features of the frontal boss. The position of *P. mukirii* obtained in the present analysis supports the hypothesis that this taxon belongs to a different evolutionary lineage in respect to the extant *Diceros* and *Ceratotherium*.

In Pandolfi (2015), *C. neumayri* and *C. simum* are phylogenetically related and *D. bicornis* is their closest relative; this topology contrasts with the hypothesis that *C. neumayri* is the common ancestor of both living species (e.g., Geraads 2005). However,

different authors considered *C. neumayri* as a convergent extra-African monophyletic lineage (cf. Giaourtsakis et al. 2009 and references therein); in this framework, a dispersal from Africa to Eurasia during the middle Miocene of an ancestor of *C. neumayri* and *D. gansuensis* has been recently proposed (Handa et al. 2017). Nevertheless, the occurrence of *Diceros* cf. *pachygnathus* (= *Ceratotherium* cf. *neumayri*) at Aragai and Ngetabkwony (Guérin 2011) could suggest an African origin of *C. neumayri*. In the present analysis, *D. gansuensis* is grouped with *P. mukirii* and *C. douariense* suggesting a relationship between these taxa that should be deeply investigated.

The position of *C. douariense* supports the paraphyly of the genus *Ceratotherium* previously proposed (Geraads 2005, 2010). *Ceratotherium douariense* has also been assigned to *Diceros* by some authors, as well as *C. neumayri*, underlying the intricate taxonomy concerning the late Miocene African species. Hooijer and Patterson (1972) considered *C. douariense* as a possible ancestor of both living African lineages.

The close relationship between *C. simum* and *C. antiquitatis* is not supported by any recent molecular analysis and could be interpreted as an artifact due to strong convergence of characters (check also Antoine 2002).

Ceratotherium primaevum is defined on a partial juvenile skull with erupting M1 (Arambourg 1959: Pl. 6, fig. 1–3) and it is also represented by a juvenile maxillae and fragments of mandibles with deciduous teeth. According to Geraads (2005), the species could be an earliest representative of forms related to *C. neumayri* and *C. douariense*. According to Giaourtsakis et al. (2009), a population similar to *C.? primaevus* (= *Diceros primaevus* in Giaourtsakis et al. 2009) would have migrated outside Africa and evolved to *Ceratotherium neumayri* (= *Diceros neumayri*); *C.? primaevum* has been also considered an ancestry for *C. douariense*.

Nevertheless, any hypothesis needs to be supported by a detailed phylogenetic analysis and additional material is needed to understand the phyletic relationship of *C.? primaevum* as well as to better understand the controversy phylogeny of the African rhinoceros clade, which is beyond the aim of this paper.

Although the studied rhinoceros is referred to a new species at present collected only from the type locality, its phylogenetic inference supports the African affinities of the land mammal assemblage of Cava Gentile and the Calabrian-Peloritan arc as a northern extension of the African continental shelf during the late Miocene. This evidence is in agreement and support previous evidences such as the occurrence of a terrestrial mammal with Afro-Arabian exclusive distribution range such as, in primis, the elephantid *Stegotetrabelodon syrticus* (Ferretti et al. 2003). The land mammal assemblage from the Cessaniti area attests in fact the existence in late Miocene times of a peculiar bioprovince in this part of the central Mediterranean typified by the co-occurrence of elements with both Afrio-Arabian and Pikermian affinities (Marra et al. 2011, 2017; Ferretti et al. 2003).

Conclusions

The study of the rhinoceros skull CES CG.R.001 collected from the base of Unit CG. SH2 at Cava Gentile, Cessaniti, Vibo Valentia, Southern Italy, and dated between 8.1 and 7.2 Ma, enables to recognize the presence of a new taxon,

'*Ceratotherium*' *advenientis* sp. nov. The holotype and only specimen assigned to this taxon clearly differs from the late Miocene European species belonging to the genus *Dihoplus* (*D. schleiermacheri, D. pikermiensis* and '*D.*' *megarhinus*) and from the 'extra-African' dicerotines *C. neumayri* and *D. gansuensis*. It also differs from the late Miocene African species *P. mukirii, C. douariense* and *C.? primaevum*, in particular by the dimensions and morphology of the neurocranial portion. The cladistic analysis places '*Ceratotherium*' *advenientis* within Rhinocerotina, and relates it to the African genera *Diceros* and *Ceratotherium*. Nevertheless, the analysis is mainly based on dental characters (130 on 214 cranial characters), suggesting that the discovery of dental material from Cava Gentile will be useful to better clarify the phylogenetic position of '*Ceratotherium*' *advenientis* and its relationships within the African clade, even if recent findings evidenced that teeth are the most evolvable structure in rhino crania as response to dietary regime in respect to the cranial shape, which is much more phylogenetically constrained (Pandolfi and Maiorino 2016 and references therein).

ORCID

Luca Pandolfi   http://orcid.org/0000-0002-4186-4126
Lorenzo Rook   http://orcid.org/0000-0001-8923-5428

References

Adams DC, Rohlf FJ, Slice DE. 2004. Geometric morphometrics: ten years of progress following the 'revolution'. Ital J Zool. 71:5–16.

Antoine P-O. 2002. Phylogénie et évolution des Elasmotheriina (Mammalia, Rhinocerotidae). Mém Mus Natl Hist Nat. 188:1–359.

Antoine P-O. 2003. Middle Miocene elasmotheriine Rhinocerotidae from China and Mongolia: taxonomic revision and phylogenetic relationships. Zool Scr. 32:95–118.

Antoine P-O, Saraç G. 2005. Rhinocerotidae (Mammalia, Perissodactyla) from the late Miocene of Akkaşdaǧi, Turkey. In: Sen S, editor. Geology, mammals and environments at Akkaşdaǧi, late Miocene of Central Anatolia. Vol. 27. Muséum national d'Histoire naturelle, Paris: Geodiversitas; p. 601–632.

Antoine PO, Downing KF, Crochet JY, Duranthon F, Flynn LJ, Marivaux L, Metais G, Rajpar ARRoohi G. 2010. A revision of aceratherium blanfordi lydekker, 1884 (mammalia: rhinocerotidae) from the early miocene of pakistan: postcranials as a key. Zoological Journal of the Linnean Society. 160:139–194.

Antoine P-O, Duranthon F, Welcomme JL. 2003. *Alicornops* (Mammalia, Rhinocerotidae) dans le Miocène supérieur des Collines Bugti (Balouchistan, Pakistan): implications phylogénétiques. Geodiversitas. 25:575–603.

Antoine PO, Orliac MJ, Atici G, Ulusoy I, Sen E, Cubukcu HE, Albayrak E, Oyal N, Aydar E, Sen S. 2012. A rhinocerotid skull cooked-to-death in a 9.2 ma-old ignimbrite flow of turkey. PLos ONE. 7(11):1–12. doi: e49997. 10.1371/journal.pone.0049997.

Arambourg C. 1959. Vertébrés continentaux da Miocène supérieur de l'Afrique du Nord. Serv Carte Géol Alg Mém. 4:5–159.

Bernor RL, Heissig K, Tobien H. 1987. Early Pliocene Perissodactyla from Sahabi, Libya. In: Boaz NT, de Heinzelin J, Gaziry W, El-Arnauti A, editors. Neogene Geology and Paleontology of Sahabi. New York: A. Liss; p. 233–254.

Bookstein FL. 1986. Size and shape spaces for landmark data in two dimensions. Stat Sci. 1:181–222.

Bookstein FL. 1991. Morphometric Tools for Landmark Data: geometry and Biology. Cambridge (New York): Cambridge University Press; p. 456.

Bookstein FL, Streissguth AP, Sampson PD, Connor PD, Barr HM. 2002. Corpus callosum shape and neuropsychological deficits in adult males with heavy fetal alcohol exposure. NeuroImage. 15:233–251.

Carone G, Domning DP. 2007. *Metaxytherium serresii* (Mammalia: sirenia): new pre-Pliocene record, and implications for Mediterranean paleoecology before and after the Messinian Salinity Crisis. B Soc Paleontol Ital. 46:55–92.

Carone G, Domning DP, Marra AC. 2013. New finds of metaxytherium serresii (gervais, 1847) (Mammalia: Sirenia) from the upper miocene of monte poro (Calabria, Italy). Boll. Soc. Paleontol. Ita. 52:187–196.

Cerdeño E. 1992. Spanish Neogene rhinoceroses. Paleontology. 35:297–308.

Cerdeño E. 1995. Cladistic analysis of the family Rhinocerotidae (Perissodactyla). Am Mus Novit. 3143:1–25.

De Christol J. 1834. Recherches sur les caractères des grandes espèces de Rhinocéros fossiles. Ann Sci Nat Paris S. 2(4):44–112.

Del Campana D. 1924. Un nuovo resto di Sirenoide del Miocene superiore della provincia di Catanzaro. Riv ital Paleontol S. 30:53–55.

Deng T. 2007. Skull of *Parelasmotherium* (Perissodactyla, Rhinocerotidae) from the Upper Miocene in the Linxia Basin (Gansu, China). J Vertebr Paleontol. 27(2):467–475.

Deng T. 2008. A new elasmothere (Perissodactyla, Rhinocerotidae) from the late Miocene of the Linxia Basin in Gansu, China. Geobios. 41:719–728.

Deng T, Qiu Z-X. 2007. First discovery of *Diceros* (Perissodactyla, Rhinocerotidae) in China. Vertebrata PalAsiatica. 45(4):287–306. [Chinese 287–300; English 301–306]

Ferretti MP, Rook L, Carone G, Marra AC. 2003. New findings of *Stegotetrabelodon syrticus* from the Late Miocene of Cessaniti, Southern Italy. B Soc Paleontol Ital. 56:89–92.

Ferretti MP, Rook L, Torre D. 2003. *Stegotetrabelodon* (Proboscidea, Elephantidae) from the Late Miocene of Southern Italy. J Vertebr Paleontol. 23:659–666.

Forsyth-Major CJ. 1888. Sur un gisement d'ossements fossiles dans l'ile de Samos, contemporain de l'age de Pikermi. C R Acad Sci. 107:1178–1182.

Geraads D. 1986. Sur les relations phyletiques de *Dicerorhinus primaevus* Arambourg, 1959, rhinoceros du Vallesien d'Algerie. C R Seanc Acad Sci Paris S 2. 102(13):835–837.

Geraads D. 1988. Révision des Rhinocerotidae (Mammalia) du Turolien de Pikermi: comparaison avec les formes voisines. Ann Paléontol. 74:13–41.

Geraads D. 1989. Vertebres fossiles du Miocene Superieur du Djebel Krechem et Artsouma (Tunisie Centrale): comparaisons biostratigraphiques. Geobios. 22(6):777–801.

Geraads D. 2005. Pliocene Rhinocerotidae (Mammalia) from Hadar and Dikika (lower Awash, Ethiopia), and a revision of the origin of modern African rhinos. J Vertebr Paleontol. 25(2):451–461.

Geraads D. 2010. Rhinocerotidae. In: Werdelin L, Sanders WJ, editors. Cenozoic Mammals of Africa. Berkeley: University of California Press; p. 669–683.

Geraads D, Alemseged Z, Bellon H. 2002. The late Miocene mammalian fauna of Chorora, Awash basin, Ethiopia: systematics, biochronology and 40K-40Ar ages of the associated volcanics. Tert Res. 21(1–4):113–122.

Geraads D, Spassov N. 2009. Rhinocerotidae (Mammalia) from the Late Miocene of Bulgaria. Palaeontogr Abt A. 287:99–122.

Giaourtsakis IX, Pehlevan C, Haile-Selassie Y. 2009. Rhinocerotidae. In: Haile-Selassie Y, Wolde-Gabriel G, editors. Ardipithecus kadabba: late Miocene Evidence from the Middle Awash, Ethiopia. Oakland: University California Press; p. 429–468.

Giaourtsakis IX. 2009. The Late Miocene mammal fauna of the Mytilinii Basin, Samos Island, Greece: new Collection 9. Rhinocerotidae. Beitr Paläontol. 31:157–187.

Giaourtsakis IX, Theodorou G, Roussiakis S, Athanassiou A, Iliopoulos G. 2006. Late Miocene horned rhinoceroses (Rhinocerotinae, Mammalia) from Kerassia (Euboea, Greece). Neues Jahrb Geol Paläontol Abh. 239(3):367–398.

Gramigna P, Bassi D, Russo F. 2012. An upper Miocene siliciclastic-carbonate ramp: depositional architecture, facies distribution, and diagenetic history (Capo Vaticano area, southern Italy). Facies. 58:191–215.

Gray JE. 1821. On the natural arrangement of vertebrose animals. *London Med Repo*. 15:296–310.

Gray JE. 1868. Observations on the preserved specimens and skeletons of the Rhinocerotidae in the collection of the British Museum and Royal College of Surgeons, including the description of three new species. Proc Zool Soc London. 1867:1003–1032.

Guérin C. 1966. *Diceros douariensis* nov. sp., un Rhinocéros du Mio–pliocène de Tunisie du Nord. Doc Lab Géol Fac Sci Lyon. 16:1–50.

Guérin C. 1976. Les restes de Rhinocéros du gisement miocène de Béni Mellal, Maroc. Géologie Méditerranéenne, Marseille. 3(2):105–107.

Guérin C. 1980. Les rhinocéros (Mammalia, Perissodactyla) du Miocène terminal au Pleistocène supérieur en Europe occidentale: comparaison avec les espèces actuelles. Doc Lab Géol Fac Sci Lyon. 79:1–1182.

Guérin C. 2000. The Neogene rhinoceroses of Namibia. Palaeontol Afr. 36:119–138.

Guérin C. 2011. Les Rhinocerotidae (Mammalia, Perissodactyla) miocènes et pliocènes des Tugen Hills (Kénya). Estud Geol. 67 (2):333–362.

Guido A, Marra AC, Mastandrea A, Tosti F, Russo F. 2012. Micromorphological, geochemical, and diagenetic characterization of sirenian ribs preserved in the late Miocene paleontological site of Cessaniti (southern Calabria, Italy). Facies. 58:179–190.

Handa N, Nakatsukasa M, Kunimatsu Y, Nakaya H. 2017. Additional specimens of *Diceros* (Perissodactyla, Rhinocerotidae) from the Upper Miocene Nakali Formation in Nakali, central Kenya. Hist Biol. 1–12. doi:10.1080/08912963.2017.1362560.

Heissig K. 1996. The stratigraphical range of fossil rhinoceroses in the late Neogene of Europe and Eastern Mediterranean. In: Bernor RL, Fahlbush V, Mittman H-W, editors. The Evolution of Western Eurasian Neogene Mammal Faunas. New York: Columbia University Press; p. 339–347.

Heissig K. 1999. Family Rhinocerotidae. In: Rössner GE, Heissig K, editors. The Miocene Land Mammals of Europe. Munich: Pfeil; p. 175–188.

Hooijer DA. 1946. Notes On Some Pontian Mammals From Sicily, Figured By Seguenza. Arch Néerl Zool. 7(3):301–333.

Hooijer DA. 1968. A rhinoceros from the Late Miocene of Fort Ternan, Kenya. Zool Med Leiden. 43(6):77–92.

Hooijer DA, Patterson B. 1972. Rhinoceroses from the Pliocene of Northwestern Kenya. Bull Mus Comp Zool Harvard University. 144 (1):1–26.

Kaup -J-J. 1832. Über Rhinoceros incisivus Cuvier und eine neue Art. Rhinoceros Schleiermacheri. Isis. 8:898–904.

Koufos GD, Kostopoulos DS, Vlachou TD. 2016. Revision of the Nikiti 1 (NKT) fauna with description of new material. In: Koufos GD, Kostopoulos DS, editors. Palaeontology of the upper Miocene vertebrate localities of Nikiti (Chalkidiki Peninsula, Macedonia, Greece). Geobios. 49(1–2):11–22.

Koufos GD. 2016. Rhinocerotidae. In: Koufos GD, Kostopoulos DS, editors. Palaeontology of the upper Miocene vertebrate localities of Nikiti (Chalkidiki Peninsula, Macedonia, Greece). Geobios. 49 (1–2):69–73.

Linnaeus C. 1758. Systema naturae per regna tria naturae, secundum classes, ordines, genera, species, cum characteribus, differentiis, synonymis, locis Editio decima, reformata. Holmiae, Laurentii Salvii. 1:1–824.

Lu X. 2013. A juvenile skull of Acerorhinus yuanmouensis (Mammalia: rhinocerotidae) from the late Miocene hominoid fauna of the Yuanmou Basin (Yunnan, China). Geobios. 46:539–548.

Lu X, Zheng X, Sullivan C, Tan J. 2016. A skull of Plesiaceratherium gracile (Rhinocerotidae, Perissodactyla) from a new lower Miocene locality in Shandong Province, China, and the phylogenetic position of Plesiaceratherium. J Vertebr Paleontol. 36(3):e1095201 (9 pages).

Marcus LF, Hingst-Zaher E, Zaher H. 2000. Application of landmarks morphometrics to skull representing the orders of living mammals. Hystrix. 11:27–47.

Marra AC. 2018. Tragoportax cf. rugosifrons (Schlosser, 1904) from the late Miocene of Cessaniti (Southern Italy). C R Palévol. 17:378–387.

Marra AC, Carone G, Agnini C, Ghinassi M, Oms O, Rook L. 2017. Stratigraphic and chronologic framework of the Upper Miocene Cessaniti succession (Vibo Valentia, Calabria, Italy). Riv Ital Paleontol S. 123:379–393.

Marra AC, Carone G, Bianucci G. 2016. Sperm whale teeth from thelate miocene of cessaniti (Southern Italy). Boll. Soc. Paleont. Ital. 55 (3):223–225.

Marra AC, Solounias N, Carone G, Rook L. 2011. Palaeogeographic significance of the giraffid remains (Mammalia, Arctiodactyla) from Cessaniti (Late Miocene, Southern Italy). Géobios. 44:189–197.

Matthew WD. 1929. Critical observations upon Siwalik mammals. Bull Mus Natl Hist Nat. 56:437–560.

Moncharmont Zei M, Moncharmont U. 1987. Il Metaxytherium medium (Desmarest) 1822 (Sirenia, Mammalia) delle arenarie tortoniane (Miocene sup.) di S. Domenica di Ricadi (Catanzaro, Italia). Mem Sci Geol. 39:285–341.

Mullin SK, Taylor PJ. 2002. The effects of parallax on geometric morphometric data. Comput Biol Med. 32:455–464.

Nakaya H, Pickford M, Yasui K, Nakano Y. 1987. Additional large mammalian fauna from the Namurungule formation, Samburu Hills, Northern Kenya. Afr Study Monogr Suppl. 5:79–129.

Neviani A. 1886. Sui giacimenti dei Cetacei fossili del monteleonese, con indicazioni di altri rinvenimenti nelle Calabrie. B Soc Geol Ital. 5:61–73.

Nicotera P. 1959. Rilevamento geologico del versante settentrionale del Monte Poro (Calabria). Memorie E Note dell'Istituto Di Geologia Applicala dell'Università Di Napoli. 7:1–92.

Ogniben L. 1973. Schema geologico della Calabria in base ai dati odierni. Geol Rom. 12:243–585.

Osborn HF. 1900. Phylogeny of the rhinoceroses of Europe. Bull Am Mus Nat Hist. 13:229–267.

Owen RM. 1848. Description of teeth and proportion of jaws of two extinct Anthracotherioid quadrupeds (Hyopotamus vectianus and Hyopotamus bovinus) discovered by the Marchioness of Hastings in the Eocene deposits on the N.W. coast of the Isle of Wight: with an attempt to develop Cuvier's idea of the classification of pachyderms by the number of their toes. Q J Geol Soc London. 4:103–141.

Pandolfi L. 2015. Persiatherium rodleri, gen. et sp. nov. (Mammalia, Rhinocerotidae), from the Late Miocene of Maragheh (Northwestern Iran). J Vertebr Paleontol. 36(1):e1040118 (8 pages).

Pandolfi L. 2018. Evolutionary history of Rhinocerotina (Mammalia, Perissodactyla). Fossilia. 2018:27–32.

Pandolfi L, Gasparik M, Magyar I. 2016. Rhinocerotidae from the Upper Miocene deposits of the Western Pannonian Basin (Hungary): implications for migration routes and biogeography. Geol Carpath. 67 (1):69–82.

Pandolfi L, Gasparik M, Piras P. 2015. Earliest occurrence of 'Dihoplus' megarhinus (Mammalia, Rhinocerotidae) in Europe (Late Miocene, Pannonian Basin, Hungary): palaeobiogeographical and biochronological implications. Ann Paléontol. 101(4):325–339.

Pandolfi L, Maiorino L. 2016. Reassessment of the largest Pleistocene rhinocerotine Rhinoceros platyrhinus (Mammalia, Rhinocerotidae) from the Upper Siwaliks (Siwalik Hills, India). J Vertebr Paleontol. 36(2):e1071266 (12 pages).

Pandolfi L, Rook L. 2017. Rhinocerotidae (Mammalia, Perissodactyla) from the latest Turolian (MN13; Late Miocene) of central and northern Italy. B Soc Paleontol Ital. 56:45–56.

Pandolfi L, Rook L. 2019. The latest miocene rhinocerotidae from sahabi (Libya). Comptes Rendus Palevol. doi:10.1016/j.crpv.2019.03.002

Pérez SI, Bernal V, González PN. 2006. Differences between sliding semi-landmark methods in geometric morphometrics, with an application to human craniofacial and dental variation. J Anat. 208:769–784.

Petrocchi C. 1941. Il giacimento fossilifero di Sahabi. B Soc Geol Ital. 60:107–114.

Piras P, Maiorino L, Raia P, Marcolini F, Salvi D, Vignoli L, Kotsakis T. 2010. Functional and phylogenetic constraints in Rhinocerotinae craniodental morphology. Evol Ecol Res. 12:897–928.

Raia P, Carotenuto F, Meloro C, Piras P, Pushkina D. 2010. The shape of contention: adaptation, history and contingency in ungulate mandibles. Evolution. 64(5):1489–1503.

Rao A, Gramigna P, Neri C. 2007. Aspetti sedimentologici e biostratigrafici della sezione Neogenica di Piscopio nell'area di M. te Poro, ViboValentia (Calabria). Geol Rom N Ser. 40:147–161.

Rohlf FJ. 2013. tpsDig2 v. 2.17. Freeware. http://life.bio.sunysb.edu/morph/

Rook L, Gallai G, Torre D. 2006. Lands and endemic mammals in the Late Miocene of Italy: contraints for palaeoegeographic outlines of Thyrrenian area. Paleogeogr Palaeoclimatol Palaeoecol. 238:263–269.

Schlager S. 2013. Morpho: calculations and visualizations related to geometric morphometrics. R package version 0.23.3. http://CRAN. R-project.org/package=Morpho

Schlosser M. 1904. Die Fossilen Cavicornia von Samos. Beitr Paläontol Geol. 17:1–118.

Seguenza L. 1902. I vertebrati fossili della Provincia di Messina-Mammiferi del Piano Pontico. B Soc Geol Ital. 21:111–174.

Seguenza L. 1907. Nuovi resti di mammiferi fossili di Gravitelli presso Messina. B Soc Geol Ital. 26:7–119.

Swofford DL. 2001. PAUP* (phylogenetic analysis using parsimony [*and other methods] version 4.0β10). Sunderland (MA): Sinauer.

Toula F. 1906. Das Gebiss und Reste der Nasenbeine von Rhinoceros (Ceratorhinus Osborn) hundsheimensis. Abhandlungen der k.k. Geologischen Reichsanstalt Wien. 20(2):1–38.

Wagner A. 1848. Urweltliche Säugetiere-Überreste aus Griechenland. Abh Bayer Akad Wiss. 5:335–378.

Zelditch ML, Swiderski DL, Sheets HD. 2012. Geometric Morphometrics for Biologists: A Primer. Amsterdam (The Netherlands): Elsevier Academic Press; p. 478 pp.

Zouhri S, Geraads D, El Boughabi S, El Harfi A. 2012. Discovery of an Upper Miocene Vertebrate fauna near Tizi N'Tadderht, Skoura, Ouarzazate Basin (Central High Atlas, Morocco). C R Palevol. 11:455–461.